

# Examination of On-Energy Shell Approximation in Two-Step $(p,n)$ Reaction

Yasushi Nakaoka

*Department of Physics  
Graduate School of Science  
University of Tokyo*

## Abstract

We examine the on-energy shell approximation applied in our previous estimation of the two-step contribution to  $(p,p')$  and  $(p,n)$  reactions. We restore the effect of absorption for the intermediate propagator in order to avoid the singularity in the transferred momentum space and calculate the numerical integration beyond the on-energy shell. We make the depth of the imaginary potential for the propagator as small as possible and guess the real two-step cross sections at zero imaginary potential.

The numerical results are already larger than those with the on-energy shell approximation at sufficiently deep imaginary potential, and they increased as the depth of the imaginary potential decreased. One obtains further contribution by including the principal part of the propagator. With this result we make a progress in solving the underestimation problem of the spin-transverse cross section.

## 1 Introduction

The multi-step processes are now essential to understand nucleon induced intermediate energy reactions. Various groups introduced the multi-step processes to explain the underestimation of the cross sections at large angles [1] or in large energy transfer regions [2]. Kawai et al. [1] determined the scattering angle dependence of the multi-step processes up to three-step processes and partly explained the underestimation of the cross sections in the one-step contribution. Investigation of multi-step processes is an interesting subject in the study of nuclear reaction mechanisms.

The two-step processes have been also applied [2] to the  $R_L/R_T$  problem in the research of spin-isospin excitations. With the random phase approximation (RPA), the spin-longitudinal response function  $R_L$  is enhanced and the peak of its energy spectrum is shifted downwards, while the spin-transverse response function  $R_T$  is quenched and its peak is shifted upwards [3]. The ratio  $R_L/R_T$  should be greater than 1 theoretically. These quantities are extracted experimentally from the measurement of the polarization

transfer coefficients [4, 5, 6, 7]. With these observables, the ratio is found to be less than 1 and this contradicts with the theoretical predictions.

The spin-longitudinal cross section  $ID_q$ , which corresponds to  $R_L$ , is roughly reproduced by distorted-wave impulse approximation (DWIA) with the RPA correlation in the lower excitation energy region, but as the excitation energy increases the theoretical results become smaller than the experimental results. In the spin-transverse cross section  $ID_p$ , which corresponds to  $R_T$ , the estimation amounts to only about half of the experimental result in the whole excitation energy region [8].

In the region where the cross sections were underestimated, Nakaoka and Ichimura [9] expected that the two-step processes have some contribution and calculated the two-step spin-longitudinal and the spin-transverse cross sections of the  $(p, n)$  reactions. We developed the formalism for two-step reactions within the framework of the plane-wave approximation to see the relative contributions from one- and two-step processes. We calculated the ratios of the sum of the one- and the two-step cross sections to the one-step cross sections and multiplied these ratios to the DWIA results and compared with the experimental results as shown in Fig. 1. We obtained the theoretical results closer to the experimental results than the DWIA results, especially for  $ID_q$ .

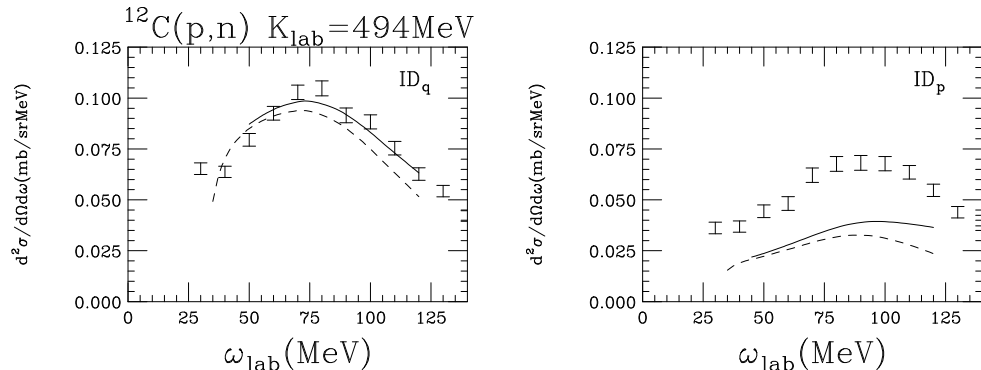


Figure 1: The DWIA calculations [8] multiplied by the ratios for the  $^{12}\text{C}(p,n)$  reactions. The left panel is the cross sections for the spin- longitudinal reactions, and the right panel is that for the spin-transverse reactions. The dashed lines indicate the DWIA results, and the solid lines indicate those multiplied by the ratios. Experimental data are taken from Ref. [6].

In this calculation we considered that the path lengths of the incident particles in the target nucleus in the one-step and the two-step processes were nearly equal, and therefore the effects of absorption in the one-step processes and in the two-step processes became nearly equal. In order to make the effect of absorption zero both in the one-step and in the two-step processes, we removed the imaginary part of the potential from the Green's function. Because of a singularity which appears to the Green's function, numerical integration was no longer executable and we had to apply the on-energy shell approximation to the Green's function. Because this approximation is not trustworthy, we here investigate the accuracy of this approximation.

In this paper, we restore the effect of absorption for the Green's function in order to avoid the singularity and calculate the numerical integration beyond the on-energy shell in the transferred momentum space. We make the depth of the imaginary potential for the propagator as small as possible and guess the real two-step cross sections at zero imaginary potential. In Sec. 2, we briefly review the formalism of the one-step and the two-step cross sections and present the method of the investigation of the on-energy shell approximation. In Sec. 3, the practical method of numerical calculation is explained. In Sec. 4, we see the result of numerical calculation. In Sec. 5, we examine the numerical results and give a justification to them. Finally we summarize this paper in Sec. 6.

## 2 Formalism

In order to recall the on-energy shell approximation which is examined in this paper, we review the formalism [9] of the one-step processes and the two-step processes in the following subsections. We consider proton induced charge exchange reactions in which the target is excited to the continuum region. The total Hamiltonian  $H$  is

$$H = H_0 + V, \quad (2.1)$$

where  $H_0$  is the unperturbed Hamiltonian and  $V$  is the residual interaction between the projectile and the target. They are

$$H_0 = H_p + U + H_T, \quad (2.2)$$

$$V = \sum_{i=1}^A v_{0i} - U \equiv \mathcal{V} - U, \quad (2.3)$$

where  $H_p$  and  $H_T$  are the projectile and the target Hamiltonian respectively, and  $v$  is the effective interaction between particles.  $U$  is the mean field that the target nucleus creates for the projectile.

### 2.1 One-step processes

Instead of calculating the two-step cross sections directly with distorted waves, we adopted a plane-wave approximation for the projectile and the ejectile. In order to see the relative importance of the one-step processes and the two-step processes, we needed to return to the one-step processes.

The one-step  $T$ -matrix is written in the  $t\rho$  approximation as

$$T_{n0}^{(1)}(\mathbf{k}_f, \mathbf{k}_i) \equiv \langle \mathbf{k}_f | \langle \Phi_n | V | \Phi_0 \rangle | \mathbf{k}_i \rangle = \langle \mathbf{k}_f | \langle \Phi_n | \mathcal{V} | \Phi_0 \rangle | \mathbf{k}_i \rangle \quad (2.4)$$

$$= t_{\text{NN}}(\mathbf{q}) \langle \Phi_n | \rho(\mathbf{q}) | \Phi_0 \rangle \quad n \neq 0, \quad (2.5)$$

where  $t_{\text{NN}}(\mathbf{q})$  is the nucleon-nucleon transition matrix (NN t-matrix),  $\rho(\mathbf{q})$  is the density operator in the momentum space.  $|\Phi_n\rangle$  are the eigenstates for the target nucleus, and  $\mathbf{q} = \mathbf{k}_f - \mathbf{k}_i$  is the momentum transfer.

The one-step cross section is written as

$$\frac{\partial^2 \sigma^{(1)}}{\partial \Omega_f \partial \epsilon_f} = K \frac{\sqrt{s}}{M_R} |t_{NN}(\mathbf{q})|^2 R(\mathbf{q}, \omega^{\text{int}}), \quad (2.6)$$

$$K \equiv \frac{\mu_i \mu_f}{(2\pi)^2} \frac{k_f}{k_i}, \quad (2.7)$$

where  $\omega^{\text{int}}$  is the energy transfer, the superscript int implies the intrinsic frame of the target,  $\mu_i$  ( $\mu_f$ ) is the reduced energy of the projectile (ejectile), and  $R(\mathbf{q}, \omega^{\text{int}})$  is the response function of the density fluctuation

$$R(\mathbf{q}, \omega^{\text{int}}) \equiv \sum_{n \neq 0} \langle \Phi_0 | \rho^\dagger(\mathbf{q}) | \Phi_n \rangle \langle \Phi_n | \rho(\mathbf{q}) | \Phi_0 \rangle \delta(\omega^{\text{int}} - E_n^{\text{int}}). \quad (2.8)$$

The quantity  $M_R (= M_T + E_n^{\text{int}})$  is the invariant mass of the residual nucleus, and  $\sqrt{s}$  is the total energy of the system.

## 2.2 Two-step processes

In the two-step processes the  $T$ -matrix is written with the intermediate state wave number  $\mathbf{k}_m$  as

$$T_{n0}^{(2)}(\mathbf{k}_f, \mathbf{k}_i) = \sum_{n' \neq 0} \int \frac{d\mathbf{k}_m}{(2\pi)^3} \langle \mathbf{k}_f | \langle \Phi_n | \mathcal{V} | \Phi_{n'} \rangle | \mathbf{k}_m \rangle G(\mathbf{k}_m) \langle \mathbf{k}_m | \langle \Phi_{n'} | \mathcal{V} | \Phi_0 \rangle | \mathbf{k}_i \rangle. \quad (2.9)$$

The excitation energy in the target nucleus was replaced with the first-step energy transfer  $\omega_1$  and the Green's function was rewritten as

$$G(\mathbf{k}_m; \omega_1) \equiv \frac{1}{E^+ - U_0 - \sqrt{M^2 + \mathbf{k}_m^2} - \sqrt{(M_T + \omega_1^{\text{int}})^2 + \mathbf{k}_m^2}}. \quad (2.10)$$

The potential  $U_0$  is a square well potential with the same depth as  $U$  and the momentum of the propagating particle does not vary during the sequential collision inside the potential  $U_0$ . It is divided into the real and imaginary parts as  $U_0 = V_0 + iW_0$ .

In fact the target gets excited after the first collision occurs, but we applied an assumption that the target is in the ground state before the second collision, and we got the double-differential cross section as

$$\begin{aligned} \frac{\partial^2 \sigma^{(2)}}{\partial \Omega_f \partial \epsilon_f} &= K \frac{s}{M_R^2} \int d\omega_1 \int \frac{d\mathbf{q}_1}{(2\pi)^3} \int \frac{d\mathbf{q}'_1}{(2\pi)^3} \\ &\times t_{NN}(\mathbf{q} - \mathbf{q}_1) t_{NN}^\dagger(\mathbf{q} - \mathbf{q}'_1) R(\mathbf{q} - \mathbf{q}_1, \mathbf{q} - \mathbf{q}'_1; \omega^{\text{int}} - \omega_1^{\text{int}}) \\ &\times G(\mathbf{k}_i + \mathbf{q}_1; \omega_1) G^*(\mathbf{k}_i + \mathbf{q}'_1; \omega_1) t_{NN}(\mathbf{q}_1) t_{NN}^\dagger(\mathbf{q}'_1) R(\mathbf{q}_1, \mathbf{q}'_1; \omega_1^{\text{int}}), \end{aligned} \quad (2.11)$$

where  $\mathbf{q}_1 \equiv \mathbf{k}_m - \mathbf{k}_i$ . The response function  $R(\mathbf{q}, \mathbf{q}'; \omega^{\text{int}})$  is expressed as

$$R(\mathbf{q}, \mathbf{q}'; \omega^{\text{int}}) = \sum_{n \neq 0} \langle \Phi_0 | \rho^\dagger(\mathbf{q}') | \Phi_n \rangle \langle \Phi_n | \rho(\mathbf{q}) | \Phi_0 \rangle \delta(\omega^{\text{int}} - E_n^{\text{int}}). \quad (2.12)$$

Here we extended the response function to a nondiagonal form with respect to the momentum transfer  $\mathbf{q}$ . The last three factors in (2.11), which is the product of two NN  $t$ -matrices and the response function, represent the first collision, and with the next product of the Green's functions, the particle in the intermediate state propagates in the target nucleus. Then the second collision occurs with the remaining three factors.

## 2.3 Spin longitudinal and transverse cross section

In this subsection we define [8] the spin-longitudinal and spin-transverse cross sections. We introduce the unit vectors

$$\hat{\mathbf{q}} = \frac{\mathbf{q}}{|\mathbf{q}|}, \quad \hat{\mathbf{n}} = \frac{\mathbf{k}_i \times \mathbf{k}_f}{|\mathbf{k}_i \times \mathbf{k}_f|}, \quad \hat{\mathbf{p}} = \hat{\mathbf{q}} \times \hat{\mathbf{n}}. \quad (2.13)$$

In this coordinate system the scattering  $T$ -matrix is written as

$$T(\mathbf{k}_f, \mathbf{k}_i) = \hat{T}_0 + \hat{T}_n \sigma_0 \cdot \hat{\mathbf{n}} + \hat{T}_q \sigma_0 \cdot \hat{\mathbf{q}} + \hat{T}_p \sigma_0 \cdot \hat{\mathbf{p}}, \quad (2.14)$$

where  $\sigma_0$  is the spin operator of the incident nucleon and the  $\hat{T}_i$  are the operators of the target.

We refer to  $ID_q$  and  $ID_p$  as the ‘spin-longitudinal’ and ‘spin-transverse’ cross sections respectively [4, 6], which are introduced by Bleszynski et al. [10] as

$$ID_q = K \text{Tr}'[\hat{T}_q \hat{T}_q^\dagger], \quad (2.15)$$

$$ID_p = K \text{Tr}'[\hat{T}_p \hat{T}_p^\dagger]. \quad (2.16)$$

Here we set the total angular momentum of the target  $J_T = 0$ . The symbol  $\text{Tr}'$  denotes the summation of all allowed initial and final states of the target,

$$\text{Tr}'[T_i T_i^\dagger] = \sum_{0,n} \langle \Phi_0 | T_i^\dagger | \Phi_n \rangle \langle \Phi_n | T_i | \Phi_0 \rangle \delta(\omega^{\text{int}} - E_n^{\text{int}}), \quad i = q, p. \quad (2.17)$$

## 2.4 Imaginary potential and absorption

The imaginary part of the potential  $W_0$  in the Green’s function represents the absorption of the propagating particle in the intermediate state. We considered that the path lengths of the incident particles in the one-step processes and the two-step processes are nearly equal, and therefore the effect of absorption in the one-step and the two-step processes become nearly equal. In the one-step processes the effect of absorption is removed by the description of the projectile and the ejectile with plane-waves. In order to make the effect of absorption zero in the two-step processes as in the one-step processes, we also removed the effect of absorption from the Green’s function.

When the imaginary part of the potential becomes zero, the Green’s function can be rewritten as

$$G(\mathbf{k}_m; \omega_1) = \mathcal{P} \frac{1}{E - V_0 - \sqrt{M^2 + \mathbf{k}_m^2} - \sqrt{(M_T + \omega_1^{\text{int}})^2 + \mathbf{k}_m^2}} - i\pi\delta\left(E - V_0 - \sqrt{M^2 + \mathbf{k}_m^2} - \sqrt{(M_T + \omega_1^{\text{int}})^2 + \mathbf{k}_m^2}\right), \quad (2.18)$$

where  $V_0$  is the real part of the potential. Neglecting the principal part of the Green’s function is the on-energy shell approximation.

The accuracy of this approximation is unknown, so we examine this approximation by calculating the seven-fold integration in (2.11) with a finite imaginary potential depth in the Green’s function. Without the effect of absorption a singularity appears to the Green’s function and the numerical integration is no longer calculable. The depth of the imaginary potential is set as small as possible, and from this result the real two-step cross section is guessed.

### 3 Numerical Calculation

In Ref. [9] we described the incident particle loses the energy  $\omega_1$  in the first collision and it propagates in the intermediate state at the energy which is smaller by  $\omega_1$  than the incident energy, but in this paper the  $\omega_1$  dependence is removed from the NN  $t$ -matrices in the second-step and the Green's functions to make the numerical calculation easier.

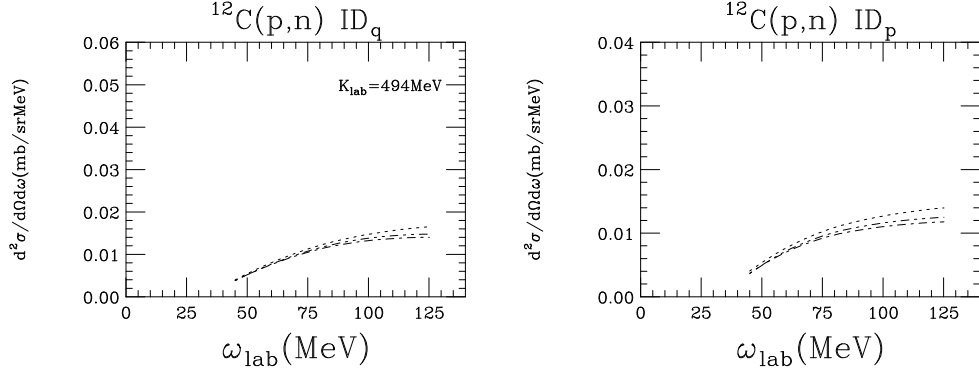


Figure 2: The dependence of the first-step energy transfer  $\omega_1$ . The dotted lines indicate the two-step cross sections with the full  $\omega_1$  dependence. The dotted-dashed lines are those without the  $\omega_1$  dependence in NN  $t$ -matrices, and the dotted-dotted-dashed lines represent the two-step cross sections without the  $\omega_1$  dependence in NN  $t$ -matrices and the Green's function respectively.

The removal of the  $\omega_1$  dependence from the NN  $t$ -matrices makes the two-step cross sections slightly decrease both in the spin-longitudinal case  $ID_q$  and in the spin-transverse case  $ID_p$  as shown in Fig. 2. Further removal of the  $\omega_1$  dependence from the Green's functions makes the two-step cross sections increase a little, but they are smaller than those with the full  $\omega_1$  dependence. It is true that the cross sections become smaller by removing the  $\omega_1$  dependence from the NN  $t$ -matrices and the Green's functions, but the differences are subtle and their behavior seem to have small effect on the examination of the on-energy shell approximation.

In Fig. 3 the integration region in the transferred momentum space is shown. Outside the spheres drawn with solid lines the values of the response functions are negligible. With this property of the response functions we restricted the integration region into the common part of two spheres. Furthermore with the delta functions introduced by the on-energy shell approximation the integration region is restricted onto the surface of the sphere drawn with a dashed line. The on-energy shell approximation is a restriction of the integration region with respect to the transferred momentum space and has nothing to do with the integration of the energy transfer  $\omega_1$ . So one can discuss the accuracy of the on-energy shell approximation in spite of the suppression of the  $\omega_1$  dependence from the NN  $t$ -matrices and the Green's functions.

The mesh sizes of the numerical integration are almost same as those in Ref. [9], although the  $z$ -axis is set parallel to the direction of  $\mathbf{q}$ .  $\Delta\omega_1^{\text{int}} = 10.0$  MeV,  $\Delta q_1^{\text{int}} = 0.2$  (1/fm), where the superscript int implies that the quantities are those in the intrinsic

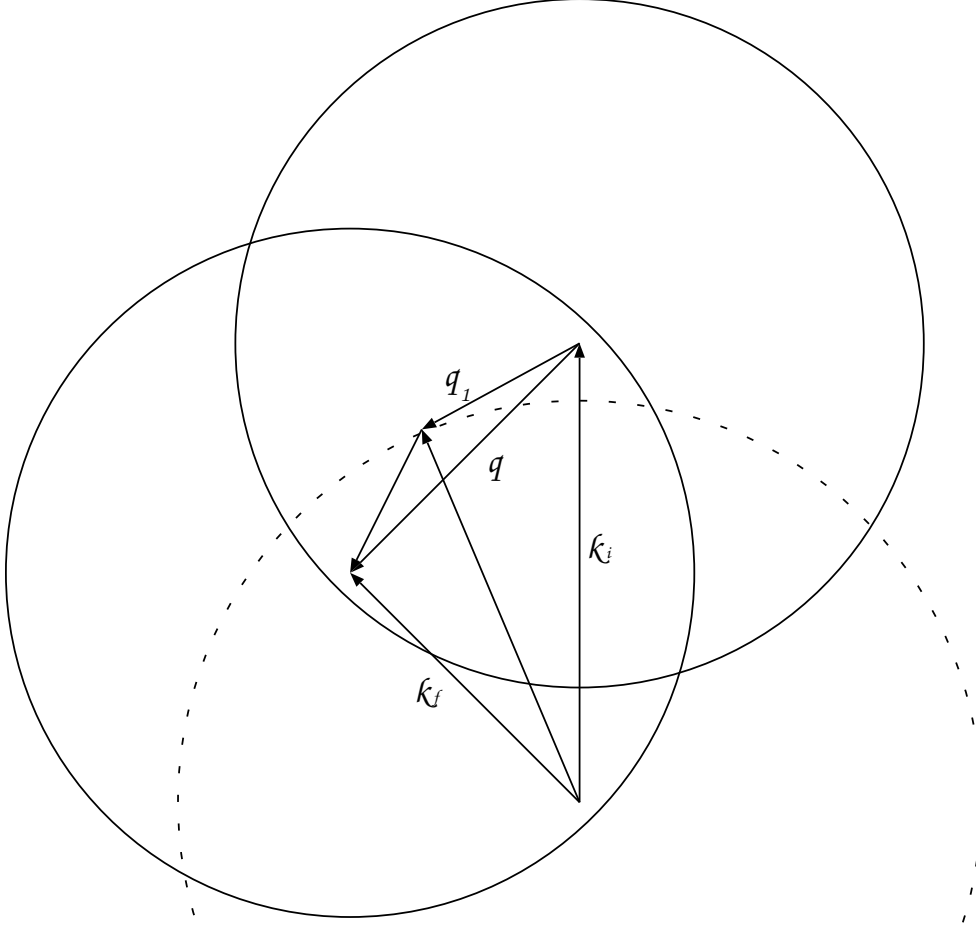


Figure 3: The integration region in the transferred momentum space. Two spheres drawn with solid lines have a radius  $4.8(1/\text{fm})$  for  $^{12}\text{C}$ , beyond which the response functions are negligible. The dashed circle is the on-energy shell on which the vector  $\mathbf{k}_m$  moves.

frame of the target.  $\Delta \cos \theta_1 = 0.125$ ,  $\Delta \phi_1 = \pi/96, \pi/48$  rad. for  $W_0 = -5.0, -10.0$  MeV respectively, and  $\Delta \phi_1 = \pi/24$  rad. for  $W_0 = -15.0, -20.0$  MeV.  $V_0 = 5.5$  MeV for  $K_{\text{lab}} = 494$  MeV.

## 4 Results

Fig. 4 is the two-step cross sections as a function of the imaginary potential depth at the energy transfer of 85 MeV. Calculations were done at  $W_0 = -20.0, -15.0, -10.0, -5.0$  MeV. We see that the two-step cross sections at  $W_0 = -20.0$  MeV are larger than those with the on-energy shell approximation. They are about 1.25 and 1.21 times of the results with the on-energy shell approximation in the  $ID_q$  case and the  $ID_p$  case respectively. The two-step cross sections become larger as the imaginary potential depth decreases. They become 1.72 times and 1.69 times at  $W_0 = -5.0$  MeV. By extrapolating these results toward  $W_0 = 0.0$  MeV, the ratios are expected to be 1.90 and 1.93 as displayed

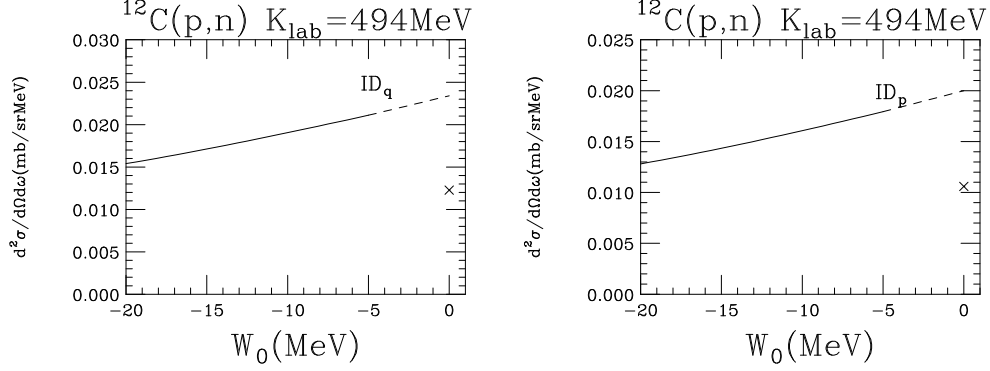


Figure 4: Two-step cross sections as a function of  $W_0$ . The energy transfer is 85 MeV. The dashed lines indicate the results extrapolated smoothly from the calculated results. The results with the on-energy shell approximation are plotted with the cross symbol at  $W_0 = 0.0$  MeV.

with dashed lines in Fig. 4.

Fig. 5 is the cross sections as a function of the energy transfer  $\omega$  at  $W_0 = -5.0$  MeV. The two-step cross sections increase as those with the on-energy shell approximation. The

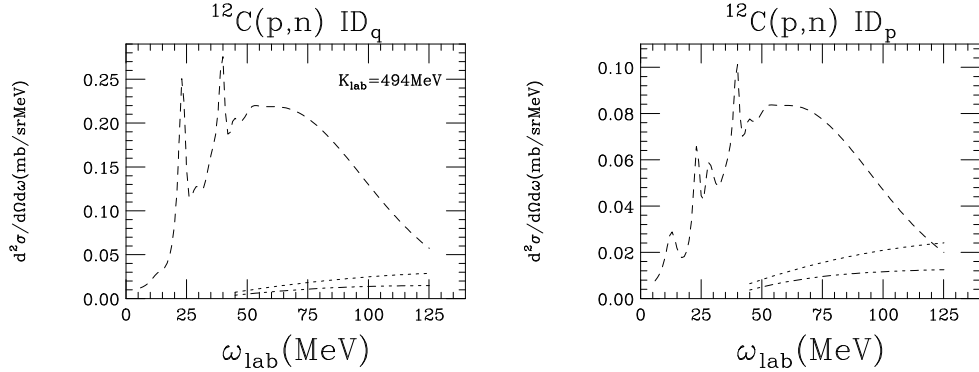


Figure 5: Two-step cross sections at  $W_0 = -5.0$  MeV. They are indicated with dotted-lines. The dotted-dotted-dashed lines are same as in Fig. 2. The dashed lines are the one-step cross sections.

ratios become 1.95 and 1.98 at  $\omega = 125$  MeV.

Taking account of these results the two-step contributions may be modified as Fig. 6. We multiply the ratios at  $W_0 = -5.0$  MeV to the original results with the on-energy shell approximation which include the  $\omega_1$  dependence in the NN  $t$ -matrices and the Green's functions. Although the numerical result becomes larger than the experimental result over the quasi-elastic peak in  $ID_q$ , the theoretical result get closer to the experimental result than the previous estimation with the on-energy shell approximation in  $ID_p$ . These results are very encouraging for explaining the underestimation of the spin-transverse cross section.



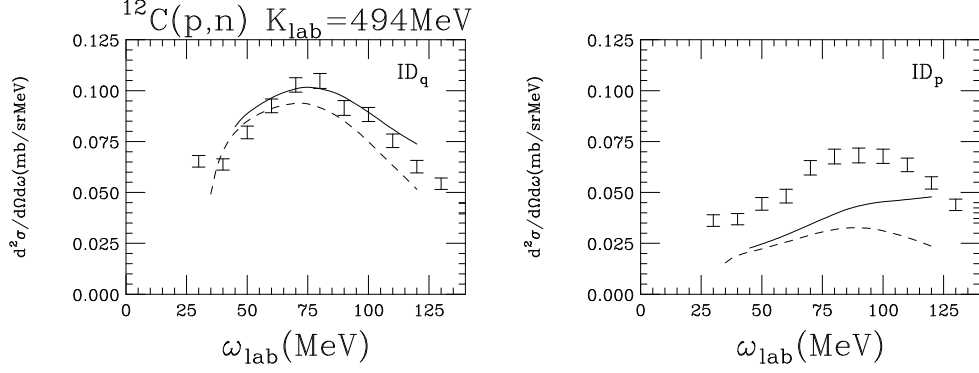


Figure 6: Same as Fig. 1, but the two-step contributions are modified.

## 5 Discussion

In this section we see a qualitative explanation of the results obtained in Sec. 4. First we consider the integration

$$\begin{aligned} \tilde{X}^{(2)}(\omega_1^{\text{int}}) &\equiv \int \frac{d\mathbf{q}_1}{(2\pi)^3} \int \frac{d\mathbf{q}'_1}{(2\pi)^3} \\ &\times t_{\text{NN}}(\mathbf{q} - \mathbf{q}_1) t_{\text{NN}}^\dagger(\mathbf{q} - \mathbf{q}'_1) R(\mathbf{q} - \mathbf{q}_1, \mathbf{q} - \mathbf{q}'_1; \omega^{\text{int}} - \omega_1^{\text{int}}) \\ &\times G(\mathbf{k}_i + \mathbf{q}_1) G^*(\mathbf{k}_i + \mathbf{q}'_1) t_{\text{NN}}(\mathbf{q}_1) t_{\text{NN}}^\dagger(\mathbf{q}'_1) R(\mathbf{q}_1, \mathbf{q}'_1; \omega_1^{\text{int}}), \end{aligned} \quad (5.1)$$

which is (2.11) but the integration with  $\omega_1$  is not included. Because the on-energy shell approximation is a restriction of the integration region in the transferred momentum space, we discuss the accuracy of the on-energy shell approximation by considering only the integration of the momentum transfers.

The quantity  $\tilde{X}^{(2)}$  has to be the square of the definite value of a complex number, because the cross section is obtained from the square of the  $T$ -matrix. Actually the response function is divided into a function of  $\mathbf{q}_1$  and a function of  $\mathbf{q}'_1$  as written in (2.12), and (5.1) is rewritten as the product of the integration of  $\mathbf{q}_1$  and its complex conjugate i.e. the integration of  $\mathbf{q}'_1$ .

Substituting (2.18) into (5.1), one gets

$$\begin{aligned} \tilde{X}^{(2)}(\omega_1^{\text{int}}) &= \int \frac{d\mathbf{q}_1}{(2\pi)^3} \int \frac{d\mathbf{q}'_1}{(2\pi)^3} \\ &\times t_{\text{NN}}(\mathbf{q} - \mathbf{q}_1) t_{\text{NN}}^\dagger(\mathbf{q} - \mathbf{q}'_1) R(\mathbf{q} - \mathbf{q}_1, \mathbf{q} - \mathbf{q}'_1; \omega^{\text{int}} - \omega_1^{\text{int}}) \\ &\times (ReG(\mathbf{k}_i + \mathbf{q}_1) ReG(\mathbf{k}_i + \mathbf{q}'_1) + i ImG(\mathbf{k}_i + \mathbf{q}_1) ReG(\mathbf{k}_i + \mathbf{q}'_1) \\ &- i ReG(\mathbf{k}_i + \mathbf{q}_1) ImG(\mathbf{k}_i + \mathbf{q}'_1) + ImG(\mathbf{k}_i + \mathbf{q}_1) ImG(\mathbf{k}_i + \mathbf{q}'_1)) \\ &\times t_{\text{NN}}(\mathbf{q}_1) t_{\text{NN}}^\dagger(\mathbf{q}'_1) R(\mathbf{q}_1, \mathbf{q}'_1; \omega_1^{\text{int}}). \end{aligned} \quad (5.2)$$

It is the fourth term which remains when the on-energy shell approximation is applied. Same argument as in the previous paragraph can be done with respect to the first term and the fourth term, and these two terms become positive respectively. Therefore the

cross sections become larger than those with the on-energy shell approximation, if it were not for the second term and the third term.

The second term and the third term are the complex conjugate of each other, and the sum gives a real number. However, the contributions to  $ID_q$  and  $ID_p$  from these terms are small, e. g. they are only  $-2.0 \times 10^{-4}$  and  $-3.2 \times 10^{-4}$  out of  $1.54 \times 10^{-2}$  mb and  $1.28 \times 10^{-2}$  mb at  $W_0 = -20.0$  MeV respectively. Thus the results of the numerical calculation in Sec. 4 became larger than those with the on-energy shell approximation.

The contributions from the fourth term in Fig. 4 are displayed in Fig. 7 with dotted lines. Their extrapolation toward  $W_0 = 0.0$  MeV seem to be the results with the on-

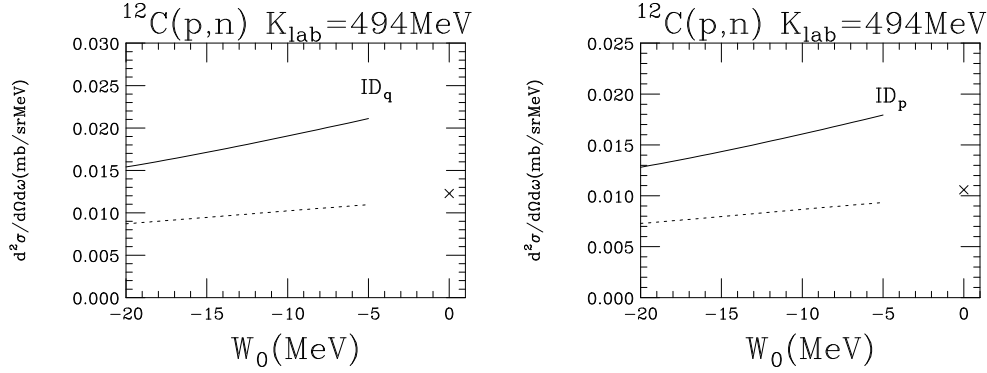


Figure 7: Same as Fig. 4, but the contributions from the fourth term are displayed with dotted lines.

energy shell approximation. This shows that the results obtained in Sec. 4 are consistent with the previous estimations with the on-energy shell approximation.

## 6 Summary

The on-energy shell approximation in Ref. [9] was examined by calculating the integration beyond the on-energy shell by restoring a finite imaginary potential. The two-step cross sections are already larger than those with the on-energy shell approximation at sufficiently deep imaginary potential, and they increased as the depth of the imaginary potential decreased. They became about two times of the results with the on-energy shell approximation at  $W_0 = -5.0$  MeV. We saw a qualitative explanation to the results and made a conclusion that the on-energy shell approximation gives an underestimation of the two-step cross sections. These results are very encouraging for explaining the underestimation of the spin-transverse cross section.

## Acknowledgement

The author would be grateful to Prof. Hideyuki Sakai, the University of Tokyo, and Prof. Munetake Ichimura, Hosei University, for useful advices.

## References

- [1] K. Ogata, M. Kawai et al., Phys. Rev. **C60**(1999), 054605
- [2] A. De Pace, Phys. Rev. Lett. **75**(1995), 29.
- [3] W.M.Alberico, M.Ericson, and A.Molinari, Nucl. Phys. **A379**(1982), 429.
- [4] J.B.McClelland et al., Phys. Rev. Lett.**69** (1992), 582.
- [5] X.Y.Chen et al., Phys. Rev. **C47**(1993), 2159.
- [6] T.N.Taddeucci et al., Phys. Rev. Lett.**73**(1994), 3516.
- [7] T. Wakasa et al., Phys. Rev. **C59**(1999), 3177.
- [8] M. Ichimura and K. Kawahigashi, Phys. Rev. **C45**(1991), 1822.
- [9] Y. Nakaoka and M. Ichimura, Prog. Theor. Phys.**102** (1999), 599.
- [10] E. Bleszynski, M. Bleszynski and C. A. Whitten, Jr., Phys. Rev.**C26**(1982),2063.